Published in final edited form as:
Dev Biol. 2010 March 1; 339(1): 141–154. doi:10.1016/j.ydbio.2009.12.026.

Evidence for an early role for BMP4 signaling in thymus and parathyroid morphogenesis

Julie Gordon[1], **Seema R. Patel**[1], **Yuji Mishina**[2], and **Nancy R. Manley**[1,*]

[1]Department of Genetics, University of Georgia, Athens, Georgia 30602

[2]University of Michigan, School of Dentistry, Ann Arbor, Michigan 48109

Abstract

The thymus and parathyroids are pharyngeal endoderm-derived organs that develop from common organ primordia, which undergo a series of morphological events resulting in separate organs in distinct locations in the embryo. Previous gene expression and functional analyses have suggested a role for BMP4 signaling in early thymus organogenesis. We have used conditional deletion of Bmp4 or Alk3 from the pharyngeal endoderm and/or the surrounding mesenchyme using Foxg1-Cre, Wnt1-Cre or Foxn1-Cre. Deleting Bmp4 from both neural crest cells (NCC) and early endoderm-derived epithelial cells in Foxg1-Cre;Bmp4 conditional mutants resulted in defects in thymus-parathyroid morphogenesis. Defects included reduced condensation of mesenchymal cells around the epithelium, partial absence of the thymic capsule, a delay in thymus and parathyroid separation, and failed or dramatically reduced organ migration. Patterning of the primordia and initial organ differentiation were not affected in any of the mutants. Deleting Bmp4 from NCC-derived mesenchyme or differentiating thymic epithelial cells (TECs) had no effects on thymus-parathyroid development, while loss of Alk3 from either neural crest cells or TECs resulted in only a mild thymic hypoplasia. These results show that the processes of cell specification and morphogenesis during thymus-parathyroid development are independently controlled, and suggest a specific temporal and spatial role for BMP4-mediated epithelial-mesenchymal interactions during early thymus and parathyroid morphogenesis.

Keywords

Bmp4; Alk3; Thymus; Parathyroid; Pharyngeal pouch; Endoderm; Mesenchyme; Organogenesis; Morphogenesis; Thymic epithelium; Foxg1-Cre; Wnt1-Cre; Foxn1-Cre

Introduction

Organogenesis comprises two distinct processes: morphogenesis, the shaping and positioning of organs; and cellular differentiation, where cells within a structure acquire specific functions. The thymus and parathyroid glands develop from common primordia, yet have distinct functions and locations within the adult: the thymus is situated above the heart and is responsible for T cell production, whereas the parathyroids are found near the thyroid gland

*Author for correspondence: nmanley@uga.edu, phone 706-542-5861, fax 706-583-0691.

and regulate calcium homeostasis. The process of thymus-parathyroid organogenesis is therefore a complex and highly organized process, involving both morphogenetic and differentiation events that must be coordinated to form structurally, functionally and spatially distinct organs.

The common thymus-parathyroid primordia form from the 3rd pair of pharyngeal pouches, outpocketings of the foregut endoderm which begin to develop at E9.5 in the mouse. Each pouch initially consists of a single epithelial cell layer surrounding a central lumen that is continuous with the pharynx. The pouch epithelium is directly surrounded by neural crest-derived mesenchyme, which is thought to be required for further proliferation and differentiation of the thymic epithelium (Auerbach, 1960; Revest et al. 2001; Itoi et al. 2007). Current evidence suggests that initial establishment of cell identity within the common primordium occurs prior to formation of the organ rudiments (Gordon et al. 2004; Liu et al. 2007). The dorsal and anterior cells express *Gcm2*, one of two mammalian orthologs of the *Drosophila glial cells missing* transcription factor (Kim et al. 1998), beginning at about E9.5, and will form the parathyroid glands (Gunther et al. 2000; Gordon et al. 2001; Liu et al. 2007). Cells in the ventral and posterior domain of the primordium will differentiate into thymic epithelial cells, and can be identified after E11 by the expression of *Foxn1* (Gordon et al. 2001), a transcription factor required cell-autonomously for thymic epithelial cell differentiation (Blackburn et al. 1996; Bleul et al., 2006). At E11-12 the epithelium proliferates, the lumen begins to close, and the resulting primordium is released from the pharynx and ectoderm via apoptosis (Gordon et al. 2004). At E12.5 the thymus and parathyroids separate from each other and begin migrating towards their final adult locations (Manley and Capecchi 1998). While the molecular mechanisms controlling patterning of the organ domains are beginning to be identified, the cellular and molecular mechanisms driving these unique morphogenetic events for the most part remain to be defined.

Bone morphogenetic proteins (BMPs) are a large family of intercellular TGF-β signaling proteins that have diverse and critical roles during embryogenesis and organogenesis, including the regulation of cell proliferation, differentiation, survival and fate (Hogan 1996). BMPs function through serine-threonine kinase receptor complexes composed of type I and type II transmembrane receptors, which in turn transduce the signal to specific Smad mediator proteins in the cytoplasm, leading to specific gene transcription in the nucleus. Bmp2 and Bmp4 preferentially signal through Bmpr-II with either Alk3 (Activin receptor-like 3, also termed Bmpr1a) or Alk6 (Bmpr1b), leading to phosphorylation of Smad-1, -5 and -8, and signal transduction. *Bmp4* is expressed in the ventral/posterior prospective *Foxn1*-expressing thymus domain of the third pharyngeal pouch and primordium from E10.5 to E12.5 and in the mesenchyme adjacent to the *Bmp4*-expressing epithelium (Moore-Scott and Manley 2005; Bleul and Boehm 2005; Patel et al. 2006). This suggests that reciprocal signaling between the two cell types may be important during this critical period of extensive morphogenetic change and cell fate determination.

We used conditional gene knockouts to define the role of Bmp4 signaling in early thymus-parathyroid organogenesis. Loss of Bmp4 from the pharyngeal endoderm and surrounding mesenchyme prior to the onset of *Foxn1* expression did not affect cell specification or differentiation, but did disrupt morphogenetic events such as lumen closure, organ separation, organ migration and formation of the mesenchymal thymic capsule, but did not affect cell specification or differentiation. Deletion of Bmp4 from either neural crest or *Foxn1*-positive thymic epithelial cells (TECs) did not affect thymus-parathyroid organogenesis, indicating temporal and spatial limits on the role for Bmp4 signaling. Finally, loss of the BMP receptor Alk3 from either TECs or neural crest cells resulted in a hypoplastic thymus with normal morphogenesis. We propose that Bmp4-mediated epithelial-mesenchymal interactions prior to the onset of *Foxn1* expression are essential for thymus and parathyroid morphogenesis.

Experimental procedures

Mice

Foxg1-Cre (Hebert and McConnell 2000), Wnt1-Cre (Danielian *et al.* 1998) or Foxn1-Cre (Gordon et al. 2007) mice were crossed to Alk3 or Bmp4 ($Bmp4^{tm1}$ or $Bmp4^{lacZ}$) null heterozygotes (Mishina et al. 1995; Dunn et al. 1997; Lawson et al. 1999). $Bmp4^{loxP}$ (Chang *et al.* 2008) or $Alk3^{fx}$ (Mishina et al. 2002) conditional alleles were maintained as homozygous colonies. Mice homozygous for both R26R (Soriano 1999) and Bmp4 conditional alleles ($Bmp4^{loxP/loxP}$;$R26R^{-/-}$) were used to assay for recombination. All mice were genotyped by PCR.

Conditional mutant embryos were generated by crossing females homozygous for the conditional allele, with or without R26R, with Cre-positive, null heterozygous males. The day of the vaginal plug was designated E0.5. Embryos carrying the tissue-specific deletion (Cre^{+};fx/null) were termed 'mutant'. All other genotypes were morphologically indistinguishable and were used as 'controls'. Genotypes were obtained by PCR of either yolk sac or embryo tail DNA as described (Dunn et al. 1997; Lawson et al. 1999; Mishina et al. 2002). All experiments were carried out with the approval of the UGA Committee for Animal Use in Research and Education.

Histology and three-dimensional reconstructions

Standard hematoxylin and eosin (H&E) staining was performed on transverse paraffin sections of embryos aged E11.5 to E13.5. Representative images are presented for each stage/genotype. At least three embryos were analyzed at each stage, one of which was chosen for three-dimensional (3D) organ reconstructions. Three embryos were used for reconstructions in the blood vessel analysis. Digital images of serial transverse H&E stained sections from a single embryo were reconstructed into a 3D image using Surf Driver™ 3.5.3 software (Surfdriver).

X-gal staining and in situ hybridization

Embryos from E9.5 to E12.5 were processed for wholemount x-gal staining as described (Gordon et al. 2001). After staining, embryos were dehydrated and embedded in paraffin wax using standard techniques. 10μm sections were cut and counterstained with eosin. X-gal staining was performed on 10μm frozen sections as described (DasGupta and Fuchs 1999). In situ hybridization for *Foxn1* and *Gcm2* was performed on paraffin sections as described (Moore-Scott and Manley 2005).

Nuclear phosphorylated-Smad 1/5/8 detection

Embryos were collected at E11.5 and fixed in 4% paraformaldehyde for 2 hours then paraffin embedded. 10μm sagittal sections were cut and immunohistochemistry was performed according to the manufacturer's instructions (Cell Signaling Technology, Inc.), using a biotinylated donkey-anti-rabbit secondary antibody (Jackson Immunoresearch). The signal was detected using the Vectastain Elite ABC (peroxidase) system (Vector Laboratories) followed by DAB (Sigma) with NiCl.

Apoptosis and proliferation assays

Apoptosis was analyzed by TUNEL assay on sagittal and transverse paraffin sections of E11.5 primordia as described (Liu et al. 2007).

Pregnant females were injected intraperitoneally with 50mg bromodeoxyuridine (BrdU, Sigma) per kg body weight. Embryos were collected 90 minutes later and snap frozen in OCT. CD45 was used to exclude proliferating lymphocytes from our analysis. 10μm sections were

fixed with ice-cold acetone for 2 minutes and treated with 2M HCl for 30 minutes before incubating with a combination of primary antibodies for 60 minutes at room temperature: rat anti-BrdU (Serotec), rabbit anti-pan-cytokeratin (DAKO) and anti-CD45-PE (Pharmingen). Sections were washed in PBS and incubated with donkey-anti-rat-FITC and donkey-anti-rabbit-cy5 secondary antibodies (Jackson Immunoresearch) for 30 minutes at room temperature. Slides were mounted using Prolong Gold Antifade reagent with DAPI (Invitrogen). Approximate cell numbers per section were counted manually: the number of $BrdU^+/CD45^+$ cells was subtracted from the total number of $BrdU^+$ cells to give the number of proliferating epithelial cells. However, after performing this analysis it was clear that the numbers of proliferating $CD45^+$ cells were very small, and made no significant difference to the final result. The primordium area on each section was measured and counts were recorded as the number of cells per 10,000μm^2. For counting $CD45^+$ cells in the LPC immigration study, only sections with an area over 10,000 μm^2 were used to ensure the main body of the primordium was being measured, and numbers were recorded as cells per section. Student's t-test was used for statistical analysis.

Immunofluorescence

Anti-CCL25 (TECK) staining was performed on 10μm frozen sections as previously described (Liu et al. 2006). Tissue was blocked in 10% donkey serum for 60 minutes before incubating with a mixture of rat anti-E-Cadherin (Zymed) and mouse anti-pan-cytokeratin (Sigma) overnight at 4°C. Sections were washed in PBS and incubated with donkey-anti-rat-FITC and donkey-anti-mouse-TR (Jackson Immunoresearch) secondary antibodies for 30 minutes at room temperature. Slides were mounted using Prolong Gold Antifade reagent with DAPI (Invitrogen).

Results

Foxg1-Cre and Wnt1-Cre activity in the pharyngeal region

To investigate the role of BMP4 signaling in early thymus development prior to the onset of Foxn1 expression at E11.25, we required a mouse strain in which Cre activity was uniform in the pharyngeal endoderm from at least E9.5. Foxg1-Cre is reported to fulfill these requirements, although it also can have variable ectopic expression (Hebert and McConnell 2000). Using the R26R lacZ reporter strain (Soriano 1999), Foxg1-Cre activity was consistently detected throughout the pharyngeal endoderm, including the third pharyngeal pouches, and in the surface ectoderm overlying the pharyngeal arches at E9.5 as previously reported (Fig. 1A-C; Hebert and McConnell 2000). However, deletion in the surrounding mesenchyme varied both between embryos and between left and right sides of a single E9.5 embryo. In some cases, mesenchymal Cre activity was similar on left and right sides (Fig. 1B), but in others there was a clear difference (Fig. 1C). This variable mesenchymal Cre activity was even more apparent in E12.5 Foxg1-Cre;Bmp4 mutants (Fig. 1D,E). In all 8 embryos of this genotype analyzed, only a small region of the surrounding mesenchyme immediately adjacent to the thymic epithelium was x-gal-positive, but the exact location of this region was variable between embryos. Thus, use of this Cre strain results in complete deletion in the third pharyngeal pouch endoderm, but variable deletion in the surrounding mesenchyme.

In contrast to Foxg1-Cre, Wnt1-Cre activity (Danielian et al. 1998) consistently marked the neural crest-derived mesenchyme and was completely absent from the pharyngeal endoderm at E10.5 (Fig. 1F,G) and E11.5 (not shown). In addition to demonstrating the location of Wnt1-Cre lineage cells, this analysis also confirms that most, if not all, of the mesenchymal cells in the region of the third pharyngeal pouch are of neural crest origin. Deletion with Wnt1-Cre should therefore efficiently remove Bmp4, or Alk3, specifically from the third pouch-associated mesenchyme.

Active Bmp signaling is present in the Foxg1-Cre;Bmp4 mutant primordium

We used an antibody against nuclear phosphorylated-smad 1/5/8 (phospho-smad) to detect active Bmp signaling in the primordium of Foxg1-Cre;Bmp4 mutant embryos and littermate controls. Even in control embryos, the intensity of the phospho-smad staining within the primordium was low relative to other regions within the embryo, such as the dorsal root ganglia (Fig. 1H,I,J), but was above background levels (Fig. 1N). Sagittal sections through the primordium of E11.5 control and mutant embryos (Fig. 1I,L) indicated phospho-smad activity both in the ventral thymus domain and the adjacent mesenchyme. Although it was not possible to quantify specific levels of Bmp signaling, there was no obvious difference between signals in control and mutant sections (n=5 embryos). Both mutants and controls showed broadly distributed low-level signal, with scattered cells within and around the primordium displaying higher levels of staining (Fig. 1I,J,L,M, white and black arrowheads). This result indicated the presence of active BMP signaling even after deletion of Bmp4.

The thymus-parathyroid primordium is smaller but patterned normally in Foxg1-Cre;Bmp4 mutants

Since *Bmp4* expression in the 3rd pouch precedes that of *Foxn1*, the transcription factor required for thymic epithelial differentiation (Moore-Scott and Manley 2005; Bleul and Boehm 2005; Patel et al. 2006), we assayed pouch formation and patterning of the thymus-parathyroid primordium in Foxg1-Cre;Bmp4 mutants (Fig. 2). At E10.5, the third pouch was of normal size and expressed the parathyroid marker *Gcm2* in the anterior, dorsal domain (Fig. 2I,J), indicating normal pouch formation and patterning. At E11.5, the second pharyngeal pouch appeared normal (Fig. 2A,B), while the third and fourth pouch derivatives were smaller than in controls (Fig. 2C-H). A small thymus-parathyroid primordium was observed in all E11.5 mutant embryos analyzed by all the different assays described in this paper. The external appearance of the embryos at E11.5 clearly showed that this phenotype was not due to an overall growth defect (Fig. 2K,L). In E11.5 Foxg1-Cre;Bmp4 mutants, the expression of both organ-specific markers *Foxn1* (Fig. 2M,N) and *Gcm2* (Fig. 2O,P) was normal, showing that correct patterning was maintained in spite of morphological differences (Fig. 2N,P asterisk). Thus, BMP4 in the early epithelium and mesenchyme is required for organ morphogenesis, but not for domain patterning through E11.5.

Normal proliferation and apoptosis in the Foxg1Cre;Bmp4 primordium at E11.5

During normal development, apoptosis is responsible for the release of the primordium from the pharynx and from the surface ectoderm at E11.75 - E12 (Gordon et al. 2004; Fig. 3A,B). At this stage in both controls and Foxg1-Cre;Bmp4 mutants, apoptotic cells were essentially confined to the contact points with the pharynx and the surface ectoderm, and little or no cell death was evident within the main body of the primordia (n=3) (Fig. 3C,D). These results demonstrated that increased apoptosis could not account for the small primordium seen in these mutants, and that the localized cell death associated with release of the primordium from the pharynx and surface ectoderm was not affected.

We used BrdU analysis to measure cell proliferation in control and mutant primordia. Surprisingly, the number of proliferating CD45^{-} stromal cells per unit area was not reduced in the Foxg1-Cre;Bmp4 mutants at E11.5 (n=3 embryos) (Fig. 3E,F,G). In both control and mutant embryos, the majority of BrdU^{+} cells were CD45^{-} and were confined to the ventral thymus domain of the primordium (Fig. 3E,F), consistent with our previous observations (Manley et al. 2004, and our unpublished data).

Taken together, these results demonstrate that the small size of the primordium at E11.5 could not be explained by a patterning defect, a reduction in proliferation or an increase in cell death.

Delayed lymphocyte colonization of the primordium at E11.5

The BrdU analysis also revealed an unexpected phenotype in the Foxg1-Cre;Bmp4 mutants. In control embryos (n=4 primordia), $CD45^+$ lymphocyte progenitor cells (LPCs) were clearly visible around the edge of the epithelium, and several cells had entered the primordium (Fig. 4A,E). However, in the mutant embryos at E11.5 there was little or no infiltration of LPCs into the primordium at E11.5 (n=4 primordia), although cells were present around the edge of the epithelium (Fig. 4B,E). At E12.5 the number of $CD45^+$ cells in the Foxg1-Cre;Bmp4 mutant thymus was similar to controls (n=4 lobes), consistent with there being a delay in their initial immigration (Fig. 4C,D,E). Since initial thymic epithelial cell patterning, as well as migration of the embryonic thymus, is independent of thymocyte-derived signals (Klug et al. 2002), it is unlikely that this delayed lymphocyte colonization is the cause of the morphogenetic defects seen in the Foxg1-Cre;Bmp4 mutant phenotype.

Colonization of the embryonic thymus by LPCs begins at E11.5, and is controlled by chemokine signaling, in particular CCL25 at this stage (Moore and Owen 1967; Liu et al. 2006). We found no obvious difference in CCL25 expression between Foxg1-Cre;Bmp4 mutants (n=6 primordia) and controls (n=6 primordia) at E11.5 (Fig. 4F,G). This correlates with the normal *Foxn1* expression at E11.5 in the Foxg1-Cre;Bmp4 mutants (Fig. 2K,L), as Foxn1 has been shown to be required for normal levels of CCL25 expression in the thymic primordium (Itoi et al. 2001; Liu et al. 2006). Furthermore, complete loss of CCL25 only reduced the number of immigrating cells, but does not delay their initial entry (Liu et al. 2006). This result therefore suggests that BMP4 signaling plays a direct or indirect role in initial LPC homing to the embryonic thymus, independently of CCL25.

Morphological changes in the thymus and parathyroids in Foxg1-Cre/Bmp4 mutants

During normal development, the common thymus-parathyroid primordium detaches from the pharynx at E12.0 and begins to migrate caudally. Soon after, the parathyroids detach from the most anterior aspect of the thymus lobes and become associated with the thyroid. The thymus lobes then continue to migrate towards the heart, where they meet at the ventral midline. In the Foxg1-Cre;Bmp4 mutants, this migration was severely disrupted. At E12.5, the thymus and parathyroid primordia on the left side of the embryo were at an anterior position consistent with little or no migration after their separation from the pharynx (Fig. 5A,B). The thymus and parathyroid primordia on the right side of the mutant embryo were also ectopic, but less so, relative to the thyroid and ultimobranchial bodies (Fig. 5A,B). This asymmetrical ectopia phenotype was seen in 100% of mutant embryos collected at this stage for all analyses performed in this study (n>25). Furthermore, both thymus lobes were on average 25% smaller in the mutants compared to the controls, while the size of the parathyroids was normal (Fig. 5A,B).

The fourth pharyngeal pouches give rise to the ultimobranchial bodies, which will become the calcitonin-producing cells of the thyroid. On E12.5 of normal development, the ultimobranchial bodies have separated from the pharynx and are located at the dorso-anterior aspect of the developing thyroid (Fig. 5A,I). In the Foxg1-Cre;Bmp4 mutant embryos, the ultimobranchial bodies had separated from the pharynx, but were 50% smaller than normal (Fig. 5B,J). In addition, the lateral lobes of the thyroid itself were absent (Fig. 5A,B).

In all Foxg1-Cre;Bmp4 mutant embryos analyzed at E13.5 (n=4) the relative organ positions were strikingly similar to that seen at E12.5, suggesting that no further migration had occurred (Fig. 5C,D,G, H,K). The thymus in the Foxg1-Cre;Bmp4 mutant embryo was still around 30% smaller than in the control embryo (Fig. 5K,L). The ultimobranchial bodies and thyroid phenotypes were also similar (Fig. 5C,D). Thus, the development of the third and fourth pharyngeal pouch-derived organs did not progress appreciably from E12.5 to E13.5, while the

mutant embryos demonstrated normal overall progression from E12.5 to E13.5, indicating that this phenotype was not the result of an arrest in embryonic development (Fig. 5O-R).

The defect in thymus migration does not correlate with abnormal arch artery remodeling

During thyroid development in mice and in zebrafish, the location of the pharyngeal arch arteries strongly influences the migration of the thyroid primordium, and defects in the carotid arteries can result in ectopic thyroid lobes (Fagman et al. 2004; Alt et al. 2006). Bmp4 is required for normal remodeling of the pharyngeal arch arteries (Liu et al. 2004), and the close association of the developing thymic lobes with the carotid arteries (Fig. 6C,J,M) suggested that organ migration defects in Foxg1-Cre;Bmp4 mutants could be secondary to an arch artery phenotype. We created a second set of 3D reconstructions to include all arteries in the region of the thymus lobes from the same E12.5 and E13.5 control and mutant embryos represented in Figure 4. Importantly, there was at least one artery present on both sides of the three mutant embryos analyzed using 3D reconstructions, and the vessels were in close association with the thymus lobes (Fig. 6D-G,K-O). In one of the E12.5 mutants, two arteries were present on the right side of the embryo (Fig. 6D,F), where the thymus lobe had migrated the furthest. On the left side of the embryo, where the thymus lobe did not migrate at all, there was only a single artery (Fig. 6D,G). In the other E12.5 mutant, and in one E13.5 embryo, the opposite arrangement was observed (Fig. 6H-O). Thus, the artery defects did not correlate with the disrupted thymus migration.

Foxg1-Cre;Bmp4 mutant TECs maintain an epithelial phenotype

Expression of the cell adhesion molecule E-Cadherin is a characteristic of all epithelial cells, and is important for their reorganization during development. E-Cadherin is under tight regulation during morphogenesis as cells undergo polarization, differentiation and migration. In particular, actively migrating epithelial cells will undergo an epithelial to mesenchymal transition (EMT) and downregulate E-Cadherin (Savagner 2001). In both the mutants and the controls, all keratin-positive epithelial cells throughout the thymus expressed E-Cadherin at both E12.5 (n=6) and E13.5 (n=2) (Fig. 6P-S). TECs also retained expression of *Foxn1* at E13.5 (Fig. 6T,U). These results indicate that the Foxg1-Cre;Bmp4 TECs did not lose their epithelial phenotype, and that TECs do not participate in active migration during normal development.

Increased apoptosis and a persistent lumen in the thymus at E12.5 and E13.5

The developing wild-type primordium contains a lumen that initially spans the length of the thymus domain. It then closes from the distal/posterior/ventral end, so that the residual lumen present at E12.5 is always at the most anterior end (Fig. 7A), and by E13.5 has closed completely (Fig. 7G). In Foxg1-Cre;Bmp4 mutant embryos this lumen was larger than normal at E12 and E12.5 (Fig. 7A,C,E,F), and was still present at E13.5 (Fig. 7H), as revealed in several different assays ($n > 10$). A long, narrow lumen stretching more than half of the developing lobe was present at E12.0, giving a slit-like appearance in transverse sections (Fig. 7C,D). In a more extreme example, the lumen at E12.5 extended throughout the length of the lobe, expanding to a large round diameter in the more posterior region (Fig. 7E, F), reminiscent of the structure of an E11.5 primordium. We further observed a stripe of increased E-cadherin levels within the E12.5 Foxg1-Cre;Bmp4 mutant thymus, that appeared to be coincident with this persistent lumen (Fig. 6R). In contrast to earlier stages (Fig. 3), TUNEL analysis performed on E12 to E13.5 embryos (n=4) revealed a dramatic increase in cells undergoing apoptosis in the mutant thymus relative to controls (Fig. 7B,D,G,H). No apoptosis was observed in the mesenchyme immediately adjacent to either mutant or control primordia (Fig. 7B,D,G,H). The majority of the apoptotic cells were clustered around the enlarged lumen (Fig. 7D,H), suggesting a possible mechanism for this phenotype.

Bmp4 is required for separation of the thymus and parathyroid and formation of the thymus capsule

The thymus and parathyroids do not separate at the correct time in Foxg1-Cre;Bmp4 mutants. At E12.5, when the two organs should be separate (Fig. 8A,C), the parathyroid was firmly attached to the thymus (Fig. 8B) and at E13.5 a small region of contact was still present (n=3) (Fig. 8F), while the control parathyroid was completely separated and adjacent to the thyroid (Fig. 8E). In the E12.5 mutants, *Gcm2*-positive parathyroid cells formed a tight cluster attached to the anterior region of the thymus, with no mixing of *Gcm2*-positive and *Gcm2*-negative cells (Fig. 8D). Thus, the cells were organized correctly in the Foxg1-Cre;Bmp4 mutants, but physical separation was progressing at a slower rate than normal. We were unable to analyze later stages due to embryonic lethality soon after E13.5.

Cranial neural crest cells surround the developing thymic lobes and form a capsule around the epithelium (Jiang et al. 2000), which is readily identifiable by histology, although no specific molecular marker has been identified. In both E12.5 and E13.5 control embryos the thymic epithelium had a distinct edge, and was surrounded by a layer of condensed mesenchyme several cells thick distinct from the less dense mesenchymal cells adjacent to it (Fig. 8G,I, bracket). In contrast, in Foxg1-Cre;Bmp4 mutants the capsule was partially disrupted at both E12.5 and E13.5 (Fig. 8H and not shown). In some areas, there was no clear border between the thymic epithelium and the surrounding mesenchyme (Fig. 8H). The disrupted thymic capsule correlated with disorganization of the surrounding mesenchyme: the boundary of morphologically identifiable capsule exactly matched that of organized versus non-organized condensing mesenchyme (Fig. 8H, arrow). The location and extent of the disrupted capsule around the circumference of each thymus lobe was variable, and this variation in mesenchyme disorganization is likely directly related to variability in Foxg1-Cre activity in these cells (Fig. 1C,D).

We noticed that the mesenchyme around the site of separation of the parathyroid and thymus was also less organized in mutants compared to controls (Fig. 8B,J). In E12.0 control embryos, just prior to detachment of the parathyroid from the thymus, the mesenchyme around the site of separation was condensed into ‘wedges’ between the parathyroid and thymus (Fig. 8J, arrows). However, in Foxg1-Cre;Bmp4 mutants at E12.5 this mesenchyme was disorganized (Fig. 8B) and the thymus and parathyroid were still physically connected (Fig. 8B,D). These results implicate a role for the mesenchyme in mediating organ separation, and point to a common BMP4-mediated mechanism for capsule formation and separation of the parathyroid from the thymus.

Tissue specificity of Bmp signaling in thymus-parathyroid morphogenesis

To further investigate the temporal and tissue-specificity of the observed phenotypes, we performed a number of tissue-specific knockouts for Bmp4 or Alk3 using either Wnt1-Cre (Danielian et al. 1998) or Foxn1-Cre (Gordon et al. 2007; Table 1). The timing of Wnt1-Cre-mediated deletion is similar to that of Foxg1-Cre, but is specific to the neural crest-derived mesenchyme (Fig. 1F,G), while Foxn1-Cre deletes within TECs, with Cre activity beginning at E11.25. These experiments allowed us to dissect which cells are producing and receiving Bmp signals, and when the signaling is occurring relevant to the observed phenotypes.

Deleting Bmp4 from neural crest-derived mesenchyme did not affect early thymus-parathyroid organogenesis (n=3) (Fig. 9A-F). This phenotype, in combination with that of the Foxg1-Cre;Bmp4 mutant, indicated that epithelial-derived Bmp4 is sufficient for morphogenesis. Initial organ formation was also unaffected in the Foxn1-Cre;Bmp4 mutants (n=4) (Fig. 9G-J), since Foxn1-Cre is expressed after cell specification has occurred. Taking into account the time of deletion and the turnover of existing Bmp4 protein, we estimate that this cross results

in loss of Bmp4 by about E12.5. Together with the data from the Foxg1-Cre;Bmp4 and Wnt1-Cre;Bmp4 mutants, these results indicate that loss of Bmp4 from the early pharyngeal epithelium prior to E12.5 is specifically responsible for the morphogenesis defects observed in the Foxg1-Cre;Bmp4 mutants, and that deletion at later stages has no obvious effects on organ migration or morphogenesis.

In a previous report, Wnt1-Cre deletion of Alk3 (Bmpr1a) specifically in neural crest cells (NCC) was shown to cause no defects in NCC formation or initial migration, but resulted in embryonic lethality around E12 (Stottmann et al. 2004). As a result, it was difficult to recover mutant embryos past E11.5. In the only E12 Wnt1-Cre;Alk3 mutant analyzed, we observed none of the morphological aspects of the Foxg1-Cre;Bmp4 mutant phenotype (Fig. 10A-D), although the thymus lobes were 30-40% smaller. Deletion of Alk3 from the epithelium at a slightly later stage with Foxn1-Cre resulted in a similar 30-40% reduction in thymic lobe size in two of three E12.5-13.5 embryos examined (Fig. 10M-T), but no other morphological defects. Two of four embryos in which Alk3 was deleted in both cell types using Foxg1-Cre also had smaller thymi with an abnormal shape (shorter in the A-P axis and wider), but did not display any of the morphogenetic defects seen in the Foxg1-Cre;Bmp4 mutants (Fig. 10E-L).

Taken together, these results suggested that while Bmp4 provided from either neural crest-derived mesenchyme or endoderm is sufficient for morphogenesis, both mesenchymal cells and thymic epithelium must be competent to receive a Bmp signal (through Alk3) in order for the thymus to reach its normal size.

Discussion

Bmp4 is required in a narrow time window for thymus-parathyroid morphogenesis

This paper represents the first detailed account of normal mouse thymus-parathyroid morphogenesis, and provides evidence for a specific and non-redundant role for BMP4-mediated epithelial-mesenchymal interactions in this process. Loss of Bmp4 from the pharyngeal epithelium and surrounding mesenchymal cells did not affect patterning, separation from the pharynx and ectoderm, or initial organ formation. However, lumen closure, initial lymphocyte colonization of the primordium, separation of the parathyroid and thymus, organization of the mesenchyme into the thymic capsule, and organ migration were all disrupted. The continued presence of phosphorylated Smad1/5/8 in these cells indicates that all aspects of the Foxg1-Cre;Bmp4 mutant phenotype occur despite continued BMP signaling in the thymus-parathyroid primordium. Deletion of Bmp4 from either NCCs or later from *Foxn1*-expressing TECs had no effect on thymus-parathyroid development, while loss of Alk3 (Bmpr1a) from either of these cell populations resulted in small but otherwise normal thymus lobes. None of the Alk3 crosses recapitulated the Foxg1-Cre;Bmp4 phenotypes, suggesting that there may be redundancy with Alk2 (ActR1) and/or Alk6 (Bmpr1b) for thymus-parathyroid morphogenesis.

Together, these results indicate that Bmp4 produced by the early (pre-Foxn1) epithelium and received by both the epithelium and the mesenchyme is essential for thymus-parathyroid morphogenesis but is not required for cell specification. Interestingly, all of the affected processes are events that normally occur after *Foxn1* expression is initiated at E11.25, despite the fact that *Bmp4* expression was blocked from at least E9.5, and none of the defects were seen in the later Foxn1-Cre knockout of Bmp4. While the need for mRNA and protein turnover after Foxn1-Cre-mediated deletion will delay functional loss of Bmp4 somewhat past E11.5, a thymus migration defect has been described in a different model following gene deletion using Foxn1-Cre (Zuklys et al. 2009). This result suggests that the lack of a phenotype after Foxn1-Cre-mediated deletion of Bmp4 does, in fact, provide evidence for a narrow time

window between 11-12.5 days for BMP4 function in thymus-parathyroid morphogenesis, and that organ migration in particular requires Bmp4 during this window.

The organ separation, lumen closure and lymphocyte colonization phenotypes in the Foxg1-Cre;Bmp4 mutant were characterized by delay rather than failure of a process. These processes were initiated and/or completed at a later time than normal, or occurred over a longer period of time to reach the same end. A delay could indicate a specific requirement for Bmp4 in these processes, or could represent a dose requirement for BMP signaling, such that a below-threshold level allows processes to occur, but at a slower rate than normal. As BMP signaling did appear to be still present despite the loss of Bmp4, it is possible that multiple BMPs could contribute to overall dose levels required for these specific aspects of morphogenesis. However, this remaining BMP signaling is not sufficient for normal morphogenesis.

While previous studies have reported roles for BMP signaling in thymus organogenesis (Bleul and Boehm 2005; Soza-Ried et al. 2008), the present study represents the first indication that Bmp4 specifically is essential for the early stages prior to the onset of Foxn1 expression.

A smaller primordium with no changes in cell death or proliferation

Organ hypoplasia could be caused by a number of mechanisms, including a smaller initial organ domain, increased apoptosis, or decreased proliferation. None of these mechanisms appear to account for the smaller E11.5 common primordia in the Foxg1-Cre;Bmp4 mutants. This phenotype is also not due to the reduction in LPCs, since very few $CD45^+$ cells are present even in the control primordium at this stage. The increase in apoptosis that we observed in the thymus at E12.5 and E13.5 could explain the smaller organ size at these stages, but not at E11.5. While steady-state proliferation was not changed, it is possible that there may be a short delay in the timing of initial epithelial cell proliferation, or that the cell cycle length was increased in the mutant epithelial cells at E11.5, so that the cells are dividing more slowly than in controls. This would not be detected by our BrdU analysis, which gives no indication of the speed with which cells are progressing through the cell cycle.

Organ ectopia reveals a left-right asymmetry in pharyngeal organ development

During mammalian embryogenesis, many internal organs display a left-right asymmetry within the embryo, and in the adult (reviewed by Levin 2005). The pharyngeal pouches are often described as bilaterally symmetrical buds on the lateral surfaces of the anterior gut tube. However, during our extensive studies of this region in both wild type and mutant embryos, we have observed slight differences between the left and right sides even during normal development. At E10.5, the left side third pouch in wild-type embryos is considerably smaller than the right side (Patel et al. 2006). Our current and previous data (Su et al. 2001) also show that in control embryos, the separation of the parathyroid from the thymus always happens slightly earlier on the right side than on the left side.

The asymmetrical organ separation and thymus migration phenotypes in the Foxg1-Cre;Bmp4 mutants always showed the thymus lobe on the left side of the embryo significantly more anterior than the one on the right, and the separation of the parathyroid from the thymus was delayed only in this side. We propose that this phenotype represents an exaggeration of normal left-right asymmetry within the pharyngeal region. A survey of mutants with similar phenotypes revealed this to be a commonly observed phenomenon, where the left side was more severely affected than the right side, although it was rarely addressed directly (Manley and Capecchi 1998; Su et al. 2001; Moore-Scott and Manley, 2005; Rizzoti and Lovell-Badge, 2007). We suggest that in each case, the loss or reduction of a signal or transcription factor at a specific time in development has a differential effect on the left and right sides because they are at slightly different developmental stages. Any disruption of the expression levels of key

proteins therefore has the potential to induce apparently different effects on the left and right sides. In the case of BMP4, removing the signal during a critical time window would therefore have a different effect on the left and right primordia, exaggerating a normally minor asymmetry and thus producing the phenotype seen in these embryos.

Interestingly, third pharyngeal pouch anomalies occur naturally in humans, and do so almost exclusively on the left side (Lin and Wang 1991; Liberman et al. 2002). In documented cases, patients complained of an enlarged neck mass, which upon examination was discovered to contain thymus and parathyroid tissue, indicative of a third pouch remnant (Miller et al. 1983; Charous et al. 2006). This lends further support to the idea that a natural left-right asymmetry exits during third pharyngeal pouch development, in both mouse and humans, which may be exaggerated under abnormal conditions, such as the Bmp4 conditional mutant phenotype presented here.

Potential mechanisms for thymus migration defects

All endoderm-derived organ primordia bud off from the primitive gut tube and undergo significant morphogenetic changes during their development. A unique characteristic of pharyngeal organs is that they also migrate from their site of origin to a different final position in the adult animal. There are three distinct mechanisms that can result in disrupted thymus migration. First, failed or delayed separation of the primordia from the pharynx is always associated with migration defects; in this case ectopia is secondary, as a tethered organ rudiment cannot migrate. Second, migration may be directly impaired, resulting in ectopic organs even if separation is normal. In the Foxg1-Cre;Bmp4 mutants, the normal separation from the pharynx indicates that the failure to migrate is a direct, functional defect. A third possibility is a change in the migratory environment, such as the correlation of thyroid migration with blood vessels (Fagman et al. 2006; Alt et al. 2006; Liu et al. 2004). However, identifying which specific tissue or function is actually defective is another matter, since the molecular and cellular mechanisms responsible for these movements during normal thymus development are unknown. The lack of a correlation between thymus migration defects and abnormal artery remodeling in the Foxg1-Cre;Bmp4 mutant embryos argues against the migration phenotype being a secondary consequence of artery defects. While it remains possible that the absence of an instructive signal from blood vessels may cause defective thymus lobe migration, our data show that the presence of these blood vessels is not sufficient to induce normal migration. Alternatively, the migration defect could be due to a failure of capsular cells to detect or respond to such a signal.

Many reports, including our own, have proposed that the neural crest-derived mesenchyme is the driving force for thymus migration. This conclusion is at least in part common sense, since the NCC-derived capsular cells cover the epithelial core of the primordium, and at an earlier stage in development are migratory. The maintenance of E-Cadherin expression in migratory thymic lobes further argues against an epithelial mechanism for migration (Savagner 2001; Fagman et al. 2003). Evidence that mesenchymal cells are required for thymus migration comes from mutant and transgenic mouse studies where NCCs were physically absent or reduced (Ohnemus et al. 2002; Wang et al. 2006), although our recent study of the Splotch mutant showed that separation from the pharynx is also delayed in the absence or reduction of neural crest (Griffith, et al. 2009). While the origin and identity of the signals driving migration or the cellular mechanisms involved are largely unknown, our data clearly implicate Bmp4 in the process. Foxg1-Cre;Bmp4 mutants showed poor condensation of mesenchymal cells around the epithelium and failure to form a complete capsule. While this did not seem to be the primary cause of the migration defect, it may be an indication of abnormal NCC differentiation. We did not see increased apoptosis in these cells, as had been previously suggested to be the cause of a thymus migration defect (Wang et al. 2006). As loss of Bmp4 from the NCC did not cause

either a capsular or a migration defect, we conclude that BMP4-mediated signaling from the epithelium to the mesenchyme is required for capsule formation and mesenchymal differentiation, and that disruption of this signal caused the Foxg1-Cre;Bmp4 mutant phenotype. Identification of the signals and cellular behaviors downstream of Bmp4 signaling will be an important key to understanding the mechanisms underlying this unusual organ migration.

Acknowledgments

We would like to thank Brigid Hogan (Duke University) for the $Bmp4^{loxP}$, $Bmp4^{tm1}$ and $Bmp4^{lacZ}$ mice, and Trevor Williams (University of Colorado) for the Foxg1-Cre mice. We also thank Yousuke Takahama (University of Tokushima) for CCL25 immunostaining advice, and Yina Li (Vanderbilt University) for experimental discussions and reagents. This work was supported by grant HD035920 from NICHD to NRM.

References

Alt B, Elsalini OA, Schrumpf P, Haufs N, Lawson ND, Schwabe GC, Mundlos S, Gruters A, Krude H, Rohr KB. Arteries define the position of the thyroid gland during its developmental relocalisation. Development 2006;133:3797–3804. [PubMed: 16968815]

Auerbach R. Morphogenetic interactions in the development of the mouse thymus gland. Dev. Biol 1960;2:271–285. [PubMed: 13795076]

Blackburn CC, Augustine CL, Li R, Harvey RP, Malin MA, Boyd RL, Miller JF, Morahan G. The nu gene acts cell-autonomously and is required for differentiation of thymic epithelial progenitors. Proc. Natl. Acad. Sci. U.S.A 1996;93:5742–5746. [PubMed: 8650163]

Bleul CC, Boehm T. Bmp signaling is required for normal thymus development. J. Immunol 2005;175:5213–5221. [PubMed: 16210626]

Chai Y, Jiang X, Ito Y, Bringas P Jr. Han J, Rowitch DH, Soriano P, McMahon AP, Sucov HM. Fate of the mammalian cranial neural crest during tooth and mandibular morphogenesis. Development 2000;127:1671–1679. [PubMed: 10725243]

Chang W, Zhengshi L, Kulessa H, Hebert J, Hogan BLM, Wu DK. Bmp4 is essential for the formation of the vestibular apparatus that detects angular head movements. PLoS Genetics 2008;4:1.

Charous DD, Charous MT, Cunnane MF, Spiegel JR. A third branchial pouch cyst presenting as a lateral neck mass in an adult. Ear, Nose Throat J 2006;85:754–757. [PubMed: 17168156]

Danielian PS, Muccino D, Rowitch DH, Micheal SK, McMahon AP. Modification of gene activity in mouse embryos in utero by a tamoxifen-inducible form of Cre recombinase. Curr. Biol 1998;8:1323–1326. [PubMed: 9843687]

DasGupta R, Fuchs E. Multiple roles for activated LEF/TCF transcription complexes during hair follicle development and differentiation. Development 1999;126:4557–4568. [PubMed: 10498690]

Dunn NR, Winnier GE, Hargett LK, Schrick JJ, Fogo AB, Hogan BLM. Haploinsufficient phenotypes in Bmp4 heterozygous null mice and modification by mutations in Gli3 and Alx4. Dev. Biol 1997;188:235–247. [PubMed: 9268572]

Fagman H, Grande M, Edsbagge H, Semb H, Nilsson M. Expression of classical cadherins in thyroid development: maintenance of an epithelial phenotype throughout organogenesis. Endocrinology 2004;144:3618–3624. [PubMed: 12865344]

Fagman H, Andersson L, Nilsson M. The developing mouse thyroid: embryonic vessel contacts and parenchymal growth pattern during specification, budding, migration, and lobulation. Dev. Dyn 2006;235:444–455. [PubMed: 16331648]

Gordon J, Bennett AR, Blackburn CC, Manley NR. Gcm2 and Foxn1 mark early parathyroid- and thymus-specific domains in the developing third pharyngeal pouch. Mech. Dev 2001;103:141–143. [PubMed: 11335122]

Gordon J, Wilson VA, Blair NF, Sheridan J, Farley A, Wilson L, Manley NR, Blackburn CC. Functional evidence for a single endodermal origin for the thymic epithelium. Nat. Immunol 2004;5:546–553. [PubMed: 15098031]

Gordon J, Xiao S, Hughes B III, Su D-M, Navarre SP, Condie BG, Manley NR. Specific expression of lacZ and cre recombinase in fetal thymic epithelial cells by multiplex gene targeting at the Foxn1 locus. BMC Dev. Biol 2007;7:69. [PubMed: 17577402]

Griffith AV, Cardenas K, Carter C, Gordon J, Iberg A, Engleka K, Epstein JA, Manley NR, Richie ER. Neural crest cells play a novel role in regulating thymus versus parathyroid fate specification of third pharyngeal pouch endoderm. Dev. Biol 327:216–227. [PubMed: 19135046]

Gunther T, Chen Z-F, Kim J, Priemel M, Rueger JM, Amling M, Moseley JM, Martin TJ, Anderson DJ, Karsenty G. Genetic ablation of parathyroid glands reveals another source of parathyroid hormone. Nature 2000;406:199–203. [PubMed: 10910362]

Hager-Theodorides AL, Outram SV, Shah DK, Sacedon R, Shrimpton RE, Vicente A, Varas A, Crompton T. Bone morphogenetic protein 2/4 signaling requires early thymocyte differentiation. J. Immunol 2002;169:5496–5504. [PubMed: 12421925]

Hebert JM, McConnell SK. Targeting of cre to the Foxg1 (BF-1) locus mediates loxP recombination in the telecephalon and other developing head structures. Dev. Biol 2000;222:296–306. [PubMed: 10837119]

Hetzer-Egger C, Schorpp M, Haas-Assenbaum A, Balling R, Peters H, Boehm T. Thymopoiesis requires Pax9 function in thymic epithelial cells. Eur. J. Immunol 2002;32:1175–1181. [PubMed: 11932925]

Hogan BL. Bone morphogenetic proteins in development. Curr. Opin. Genet. Dev 1996;6:432–438. [PubMed: 8791534]

Itoi M, Kawamoto H, Katsura Y, Amagai T. Two distinct steps of immigration of hematopoietic progenitors into the early thymus anlage. Int. Immunol 2001;13:1203–1211. [PubMed: 11526101]

Itoi M, Tsukamoto N, Yoshida H, Amagai T. Mesenchymal cells are required for functional development of thymic epithelial cells. Int. Immunol 2007;19:953–964. [PubMed: 17625108]

Jiang X, Rowitch DH, Soriano P, McMahon AP, Sucov HM. Fate of the mammalian cardiac neural crest. Development 2000;127:1607–1616. [PubMed: 10725237]

Kim J, Jones BW, Zock C, Weng H, Goodsman CS, Anderson DJ. Isolation and characterization of mammalian homologs of the Drosophila gene glial cells missing. Proc. Natl. Acad. Sci. U.S.A 1998;95:12364–12369. [PubMed: 9770492]

Klug DB, Carter C, Gimenez-Conti IB, Richie ER. Cutting edge: thymocyte-independent and thymocyte-dependent phases of epithelial patterning in the fetal thymus. J. Immunol 2002;169:2842–2845. [PubMed: 12218095]

Lawson KA, Dunn NR, Roelen BAJ, Zeinstra LM, Davis AM, Wright CVE, Korving JPWFM, Hogan BLM. Bmp4 is required for the generation of primordial germ cells in the mouse embryo. Genes Dev 1999;13:424–436. [PubMed: 10049358]

Levin M. Left-right asymmetry in embryonic development: a comprehensive review. Mech. Dev 2005;122:3–25. [PubMed: 15582774]

Liberman M, Kay S, Emil S, Flageole H, Nguyen LT, Tewfik TL, Oudjhane K, Labarge J-M. Ten years of experience with third and fourth branchial remnants. J. Pediatr. Surg 2002;37:685–690. [PubMed: 11987078]

Lin J-N, Wang K-L. Persistent third branchial apparatus. J. Pediatr. Surg 1991;26:663–665. [PubMed: 1941452]

Liu C, Saito F, Liu Z, Lei Y, Uehara S, Love P, Lipp M, Kondo S, Manley N, Takahama Y. Coordination between CCR7- and CCR9-mediated chemokine signals in prevascular fetal thymus colonization. Blood 2006;108:2531–2539. [PubMed: 16809609]

Liu W, Selever J, Wang D, Lu M-F, Moses KA, Schwartz RJ, Martin JF. Bmp4 signaling is required for outflow-tract septation and branchial arch artery remodeling. Proc. Natl. Acad. Sci. U.S.A 2004;101:4489–4494. [PubMed: 15070745]

Liu Z, Yu S, Manley NR. Gcm2 is required for the differentiation and survival of parathyroid precursor cells in the parathyroid/thymus primordia. Dev. Biol 2007;305:333–346. [PubMed: 17382312]

Manley NR, Capecchi MR. Hox group 3 paralogs regulate the development and migration of the thymus, thyroid, and parathyroid glands. Development 1998;195:1–15.

Manley NR, Selleri L, Brendolan A, Gordon J, Cleary ML. Abnormalities of caudal pharyngeal pouch development in Pbx1 knockout mice mimic loss of Hox3 paralogs. Dev. Biol 2004;276:301–312. [PubMed: 15581866]

Miller D, Hill JL, Sun CC, O'Brien DS, Haller JA Jr. The diagnosis and management of pyriform sinus fistulae in infants and young children. J. Pediatr. Surg 1983;18:377–381. [PubMed: 6620077]

Mishina Y, Suzuki A, Ueno N, Behringer RR. Bmpr encodes a type I bone morphogenetic protein receptor that is essential for gastrulation during mouse embryogenesis. Genes Dev 1995;9:3027–3037. [PubMed: 8543149]

Mishina Y, Hanks MC, Miura S, Tallquist MD, Behringer RR. Generation of Bmpr/Alk3 conditional knockout mice. genesis 2002;32:69–72. [PubMed: 11857780]

Moore MAS, Owen JJT. Experimental studies on the development of the thymus. J. Exp. Med 1967;126:715–726. [PubMed: 4861748]

Moore-Scott BA, Manley NR. Differential expression of sonic hedgehog along the anterior-posterior axis regulates patterning of pharyngeal pouch endoderm and pharyngeal endoderm-derived organs. Dev. Biol 2005;278:323–335. [PubMed: 15680353]

Ohnemus S, Kanzler B, Jerome-Majewska LA, Papaionnou VE, Boehm T, Mallo M. Aortic arch and pharyngeal phenotype in the absence of BMP-dependent neural crest in the mouse. Mech. Dev 2002;119:137–135. [PubMed: 12464427]

Revest JM, Suniara RK, Kerr K, Owen JJ, Dickson C. Development of the thymus requires signaling through the fibroblast growth factor receptor R2-IIIb. J. Immunol 2001;167:1954–1961. [PubMed: 11489975]

Rizzoti K, Lovell-Badge R. SOX3 activity during pharyngeal segmentation is required for craniofacial morphogenesis. Development 2007;134:3437–3448. [PubMed: 17728342]

Savanger P. Leaving the neighborhood: molecular mechanisms involved during epithelial-mesenchymal transition. BioEssays 2001;23:912–923. [PubMed: 11598958]

Soriano P. Generalized lacZ expression with the ROSA26 Cre reporter strain. Nat. Genet 1999;21:70–71. [PubMed: 9916792]

Soza-Ried C, Bleul C, Schorpp M, Boehm T. Maintenance of thymic epithelial phenotype requires extrinsic signals in mouse and zebrafish. J. Immunol 2008;181:5272–5277. [PubMed: 18832682]

Su D-M, Ellis S, Napier A, Lee K, Manley NR. Hoxa3 and Pax1 regulate epithelial cell death and proliferation during thymus and parathyroid organogenesis. Dev. Biol 2001;236:316–329. [PubMed: 11476574]

Wang J, Nagy A, Larsson J, Dudas M, Sucov HM, Kaartinen V. Defective ALK5 signaling in the neural crest leads to increased postmigratory neural crest cell apoptosis and severe outflow tract defects. BMC Dev. Biol 2006;6:51–64. [PubMed: 17078885]

Winnier G, Blessing M, Labowsky PA, Hogan BL. Bone morphogenetic protein-4 is required for mesoderm formation and patterning in the mouse. Genes Dev 1995;9:2105–2116. [PubMed: 7657163]

Zuklys S, Gill J, Keller MP, Hauri-Hohl M, Zhanybekova S, Balciunaite G, Na K-J, Jeker LT, Hafen K, Tsukamoto N, Amagai T, Taketo MM, Krenger W, Hollander GA. Stabilized β-catenin in thymic epithelial cells blocks thymus development and function. J. Immunol 2009;182:2997–3007. [PubMed: 19234195]

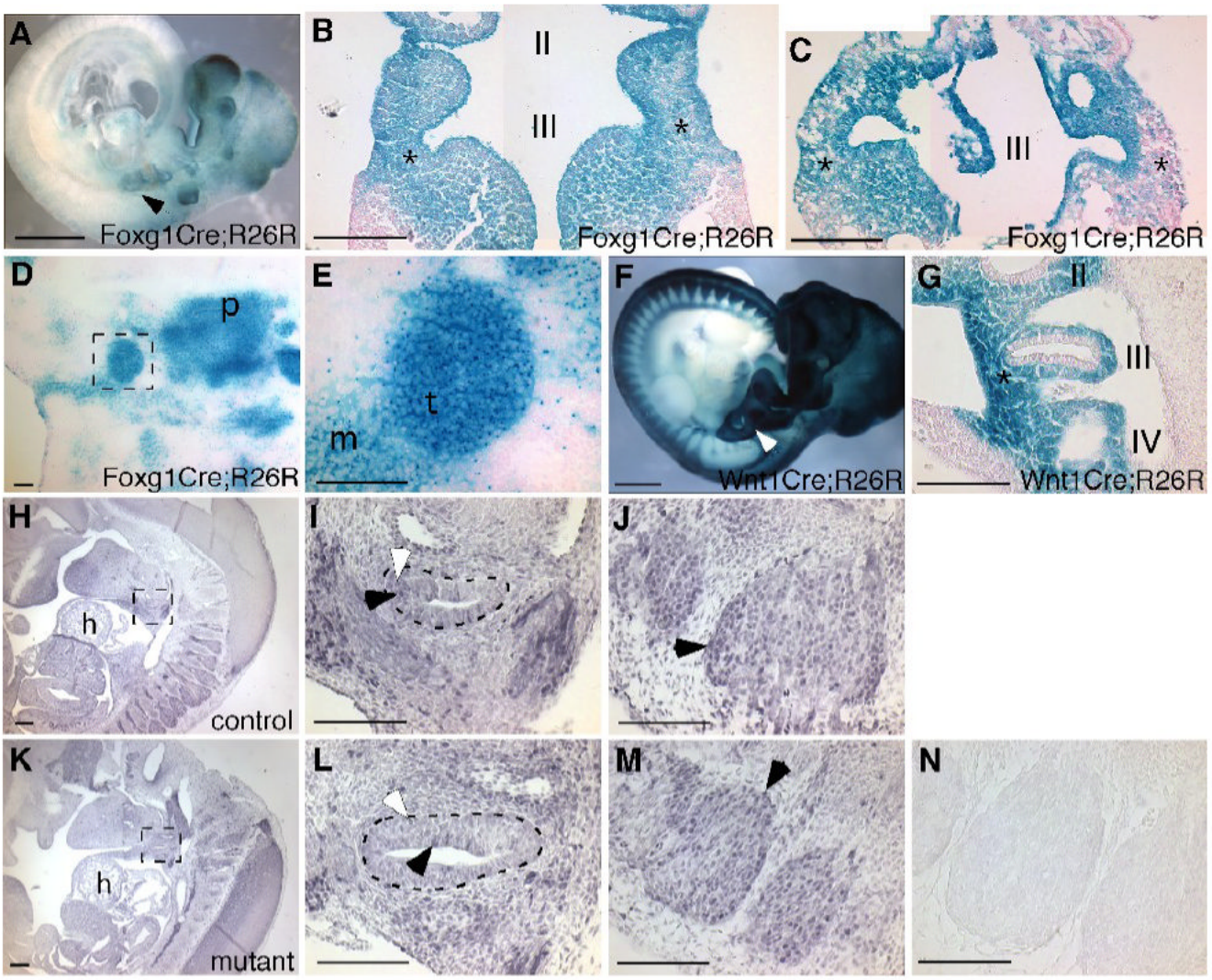

Fig. 1.

Foxg1-Cre and Wnt1-Cre activity and presence of Bmp signaling in control and mutant embryos. (A) Lateral view of an E9.5 Foxg1-Cre;R26R embryo, showing Cre activity throughout the pharyngeal region, including the 3rd pouch (arrow). (B, C) Coronal sections of two different E9.5 Foxg1-Cre;R26R embryos, showing consistent Cre activity in the 3rd pouch endoderm and surface ectoderm, but variable expression in the surrounding mesenchyme (*). Anterior is up. (D, E) Transverse sections through an E12.5 Foxg1-Cre;Bmp4;R26R embryo showing uniform Cre activity in the thymic epithelium (t) but variable activity in the adjacent mesenchyme (m). Dorsal is up. (F) Lateral view of an E10.5 Wnt1-Cre;R26R embryo, showing Cre activity in neural crest-derived cells, including those in the region of the third pharyngeal pouch (arrow). (G) Sagittal section through the embryo in (F), showing Wnt1-Cre activity in neural crest cells surrounding the third pharyngeal pouch (*), but not in the epithelium itself. Anterior is up, ventral is to the left. (H, I, J, K, L) Sagittal sections showing anti-phospho-smad staining (black) in control (H, I) and Foxg1-Cre;Bmp4 mutant (K, L) primordia. The mutant primordium in L appears larger than the control in I because of the plane of section. (J, M) Sagittal sections through the same embryos showing strong signal in the dorsal root ganglia in control (J) and mutant (M). Black arrowheads in I, J, L, M indicate stronger signal. White arrowheads in I, L indicate lower-level signal. No signal was present in the no-primary-

antibody control (N). Anterior is up, ventral is to the left. I, II, III, IV first, second, third, fourth pharyngeal pouch. p, pharynx. h, heart. Scale bar in A, F = 1mm. Scale bars in H, K = 200μm. All other scale bars = 100μm.

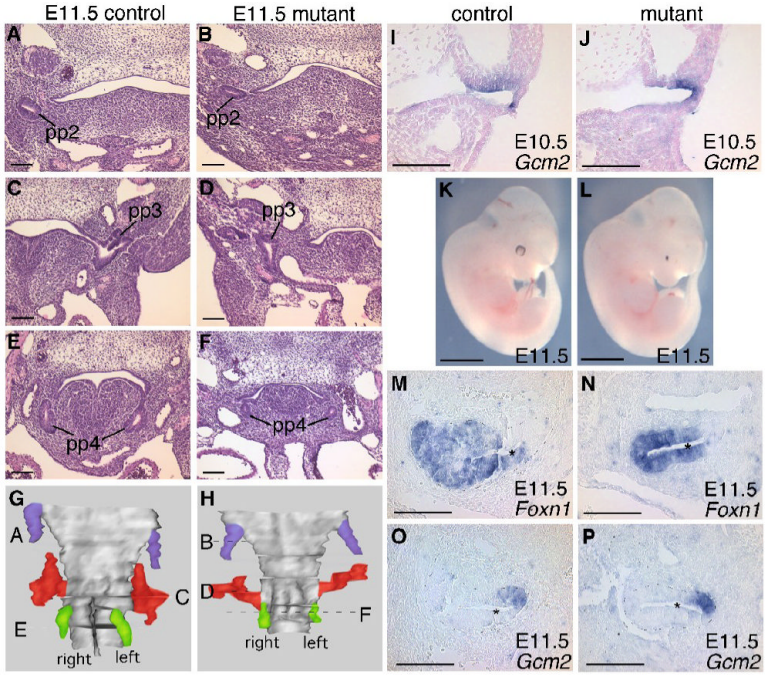

Fig. 2.

Morphology and patterning of the pharyngeal region at E10.5 and E11.5. (A-F) Transverse sections stained with H&E from control (A,C,E) and Foxg1-Cre;Bmp4 mutant (B,D,F) embryos. pp2, pp3, pp4, second, third, fourth pharyngeal pouch. Dorsal is up. (G,H) 3D reconstructions of the pharynx with the second (blue), third (red) and fourth (green) pharyngeal pouches of control (G) and Foxg1-Cre;Bmp4 mutant (H) embryos, created using the sets of sections represented in (A-F). Locations of the sections shown in A-F are indicated. (I,J) Section in situ hybridization on coronal sections for Gcm2 in control (I) and mutant (J) embryos. (K,L) Lateral views of whole E11.5 control (K) and Foxg1-Cre;Bmp4 mutant (L) embryos. Note the small eyes in the mutant. (M-P) In situ hybridization on sagittal sections for *Foxn1* and *Gcm2* in control (M,O) and mutant (N,P) embryos. * = lumen. Dorsal is up, ventral is to the left. Scale bars in K,L = 2mm. All other scale bars = 100μm.

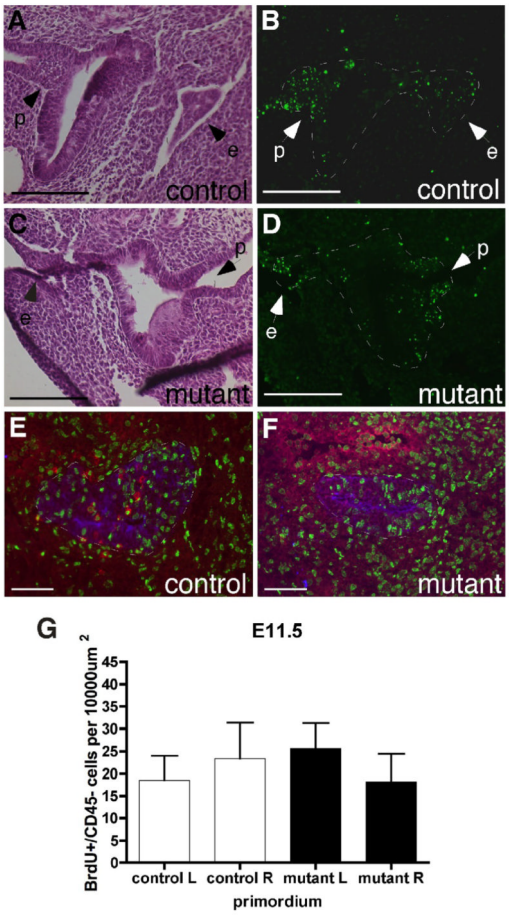

Fig. 3.

Normal proliferation and cell death at E11.5. (A-D) Adjacent transverse sections through control (A,B) and Foxg1-Cre;Bmp4 mutant (C,D) primordia. H&E stain (A,C) for morphology, TUNEL analysis (B,D) for apoptosis. e, surface ectoderm. p, attachment to the pharynx. Dorsal is up. (E,F) Sagittal sections through an E11.5 control (E) and Foxg1-Cre;Bmp4 mutant (F) primordium triple-stained for BrdU (green) CD45 (red) and pan-keratin (blue). Anterior is up and ventral is to the right. (G) Summary of $BrdU^{+}$ cell counts per section. Left (L) and right (R) sides were analyzed separately. All scale bars = 100μm.

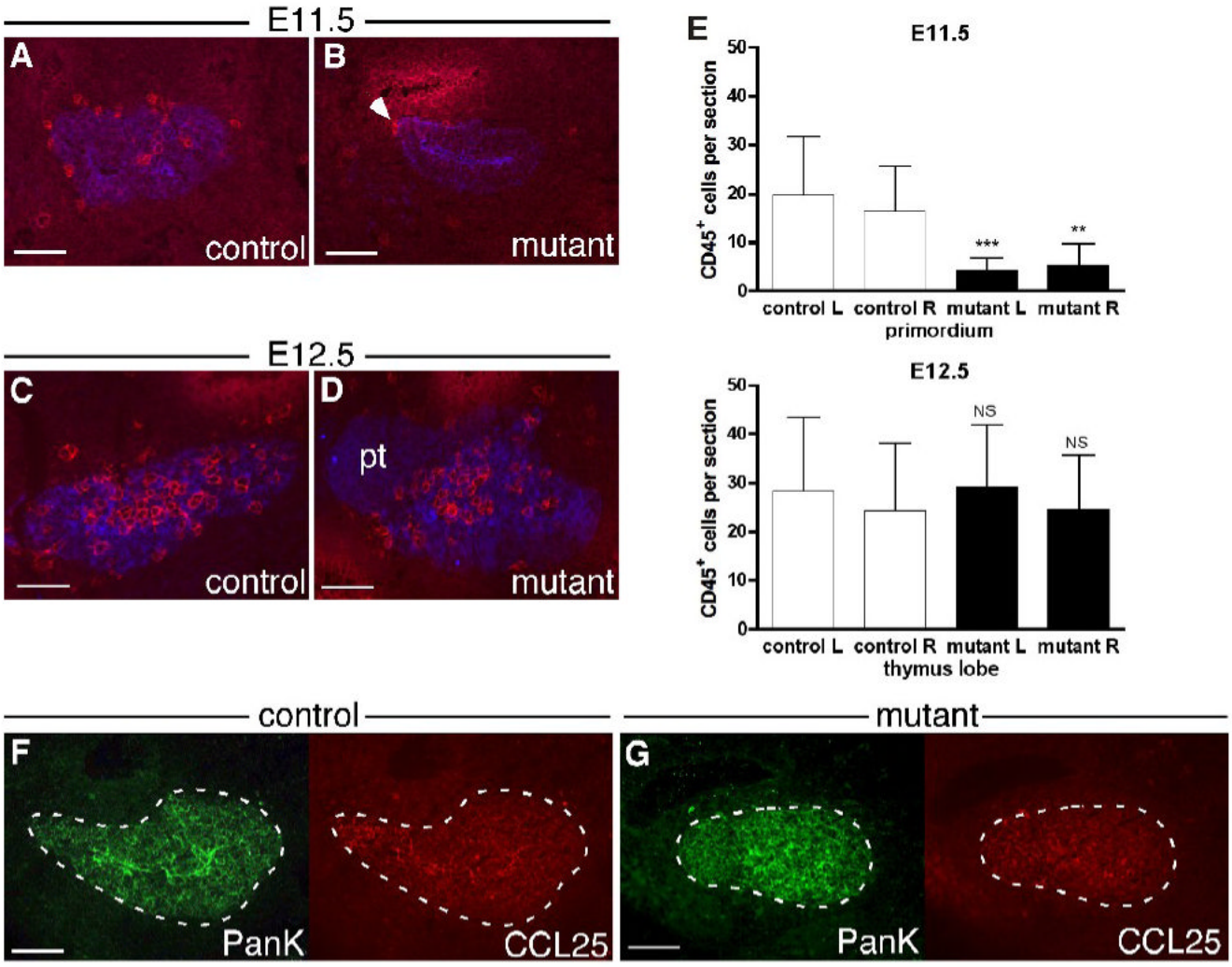

Fig. 4.

Delayed lymphocyte colonization of the Foxg1-Cre;Bmp4 mutant thymus. (A-D) Sagittal sections through E11.5 control (A) and mutant (B) primordia, and transverse sections through E12.5 control (C) and mutant (D) thymi, double-stained for CD45 (red) and pan-keratin (blue). The number of $CD45^+$ lymphocytes in the mutant primordium was reduced, with only a few cells at the dorsal end (B, arrow). (C,D) Anterior is up and ventral is to the right. (E) Summary of $CD45^+$ cell counts per section. In each case, mutant left was compared to control left and mutant right with control right. Error bars indicate SD. *** = $p < 0.001$. ** = $p < 0.01$. NS = not significant ($p > 0.05$). (F,G) Sagittal sections through E11.5 control (F) and mutant (G) primordia double-stained for CCL25 (red) and pan-keratin (green). Anterior is up and ventral is right. Scale bars = 100μm.

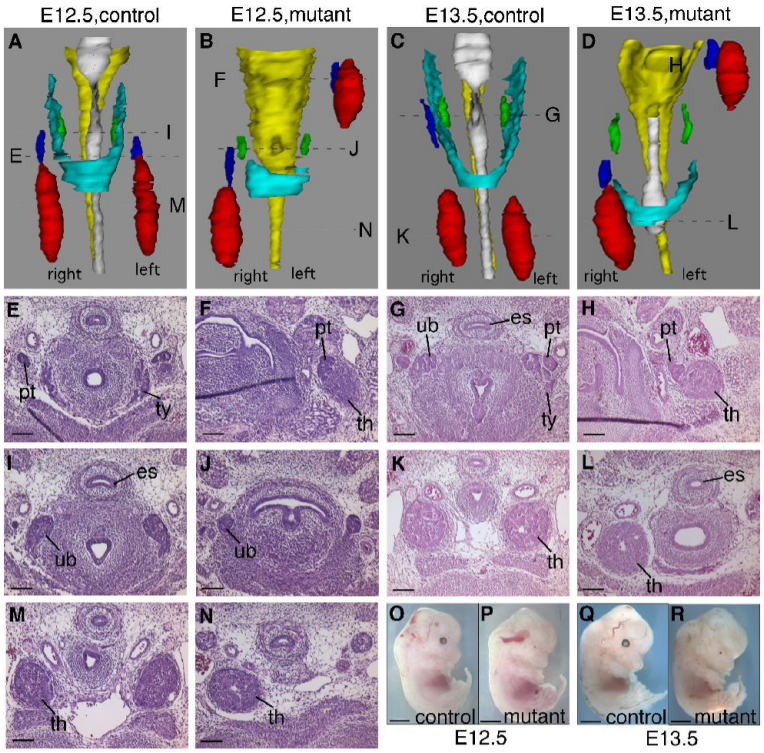

Fig. 5.

Pharyngeal organ morphology in E12.5 and E13.5 Foxg1-Cre;Bmp4 mutants. (A-D) 3D reconstructions of the pharyngeal region of E12.5 control (A), E12.5 mutant (B), E13.5 control (C) and E13.5 mutant (D) embryos, showing thymus (red), parathyroids (blue), ultimobranchial bodies (green), thyroid (cyan), esophagus (yellow) and trachea (white). Locations of the sections in the histological panels are indicated. (E,I,M) E12.5 control parathyroid (pt), thyroid (ty), ultimobranchial bodies (ub), and thymus (th). (F,J,N) E12.5 mutant parathyroid, thymus and ultimobranchial bodies. (G,H) E13.5 control parathyroid, thyroid, ultimobranchial bodies and thymus. (H,L) E13.5 mutant parathyroid and thymus. (O-R) Lateral views of whole E12.5 control (O), E12.5 mutant (P), E13.5 control (Q) and E13.5 mutant (R) embryos, showing normal developmental progression. Scale bars in O-R = 2mm. All other scale bars = 100μm.

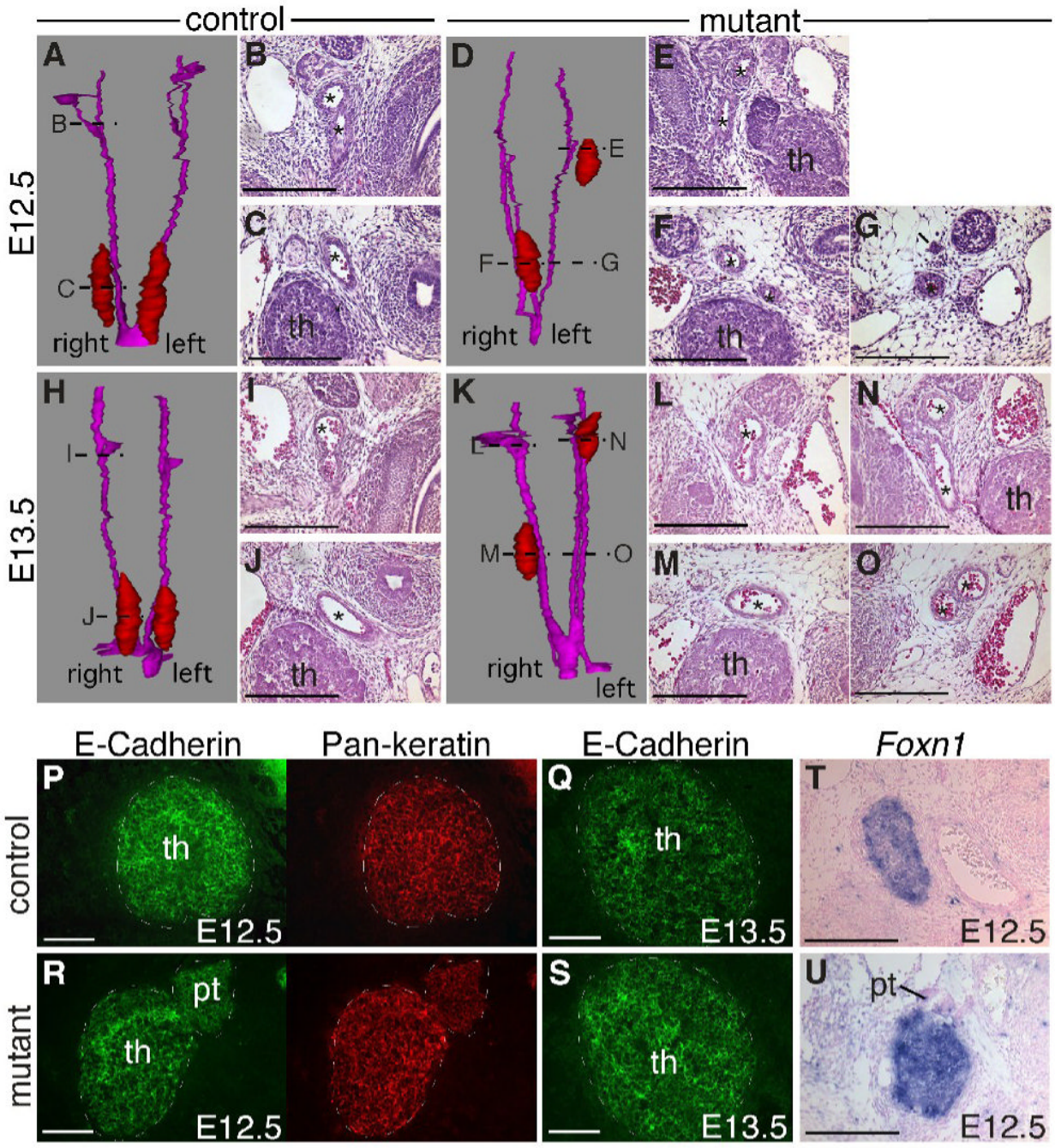

Fig. 6.

Pharyngeal arch arteries and thymic epithelial properties of Foxg1-Cre;Bmp4 mutants. (A-O) 3D reconstructions and transverse sections of E12.5 control (A-C), E12.5 mutant (D-G), E13.5 control (H-J) and E13.5 mutant (K-O) embryos. Reconstructions show the thymus (red) and the pharyngeal arteries (magenta). Locations of the sections in the histological panels are indicated. In control embryos, there was a single artery (*) adjacent to each thymus lobe, but in mutants there were often multiple arteries. (P-S) Transverse sections through E12.5 (P,R) and E13.5 (Q,S) thymus lobes double-stained for E-Cadherin (green) and pan-keratin (red). (T,U) *Foxn1* in situ hybridization performed on transverse sections of E12.5 control (T) and

mutant (U) thymus lobes. In all sections, dorsal is up. th, thymus. pt, parathyroid. Scale bars = 100μm.

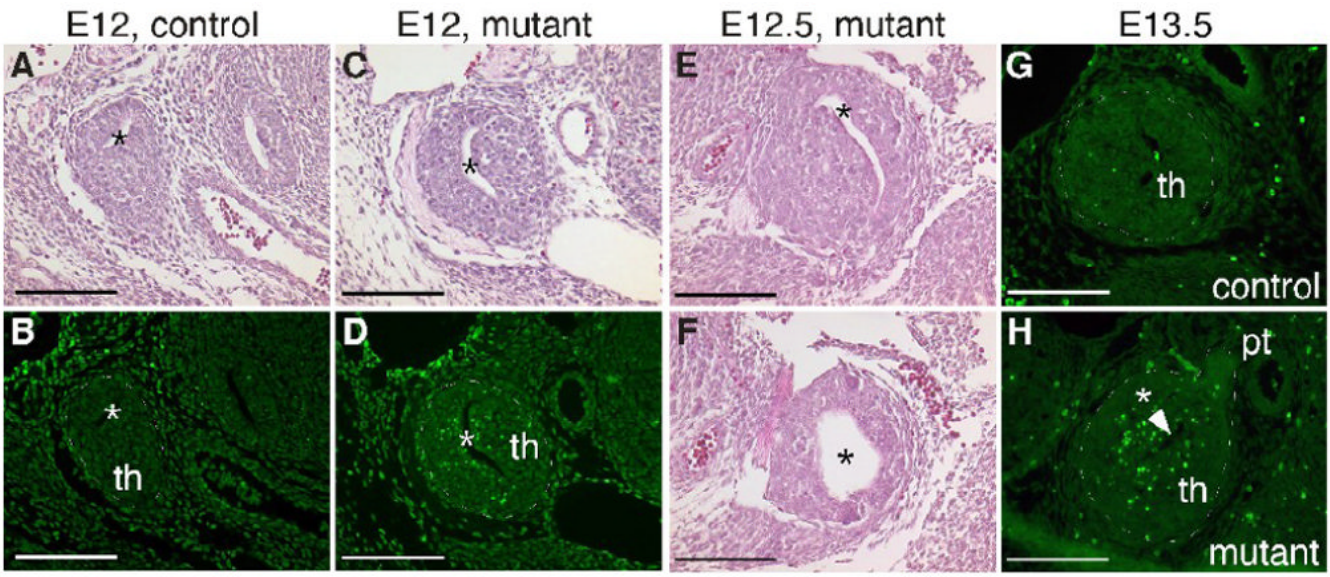

Fig. 7.

Increased apoptosis in the Foxg1-Cre;Bmp4 mutant thymus at E12.5 and E13.5. (A-D) Adjacent transverse sections through E12 control (A,B) and mutant (C,D) thymic primordia, stained with H&E (A,C) or after TUNEL analysis (B,D). Apoptosis is increased around the enlarged lumen (*) in the mutant (D). In all panels, dorsal is up and medial is to the right. (E,F) Transverse sections through the same E12.5 mutant thymus stained with H&E; (F) is more posterior than (E). (G,H) Transverse sections through an E13.5 control (G) and mutant (H) thymus following TUNEL staining. th, thymus. pt, parathyroid. Scale bar = 100μm.

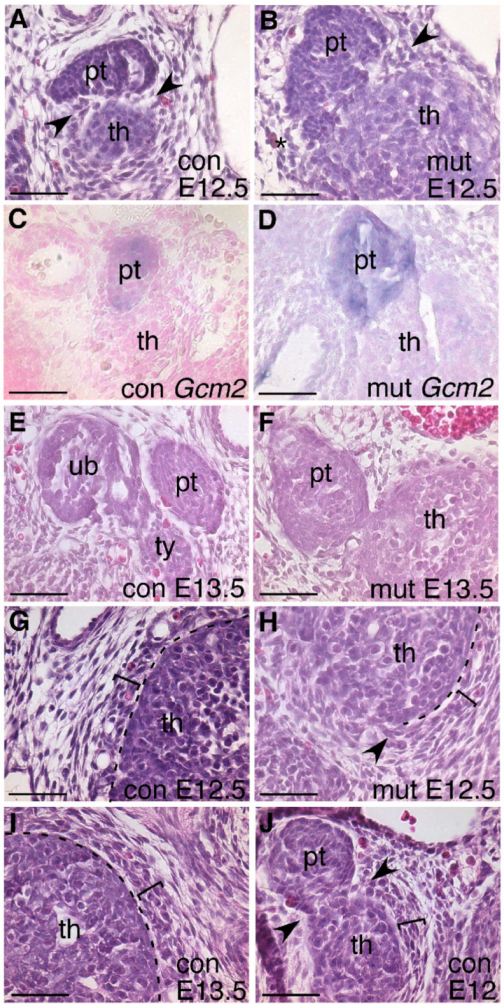

Fig. 8.

Disrupted mesenchymal condensation and delayed separation of the thymus and parathyroid in Foxg1-Cre;Bmp4 mutants. (A,B,G,H) H&E stained transverse sections through E12.5 control (A,G) and Foxg1-Cre;Bmp4 mutant (B,H) embryos. (C,D) *Gcm2* expression at E12.5 in control (C) and mutant (D) embryos. (E,F,I) E13.5 transverse sections stained with H&E. At E12.5 and E13.5 the condensing mesenchyme (bracket) and thymus capsule (dotted line) are clearly evident (G,I). Part of the thymus capsule is missing in the mutant (H), coincident with adjacent mesenchymal disorganization (arrow). In controls at E12 and E12.5 (J,A), the mesenchyme at the site of parathyroid-thymus separation condenses to form ‘wedges’ (arrows). (B) E12.5 mutant with some organization into a ‘wedge’ on one side (arrow), but not on the other (*). con, control. mut, mutant. th, thymus. pt, parathyroid. ub, ultimobranchial body. ty, thyroid. Scale bars = 50μm.

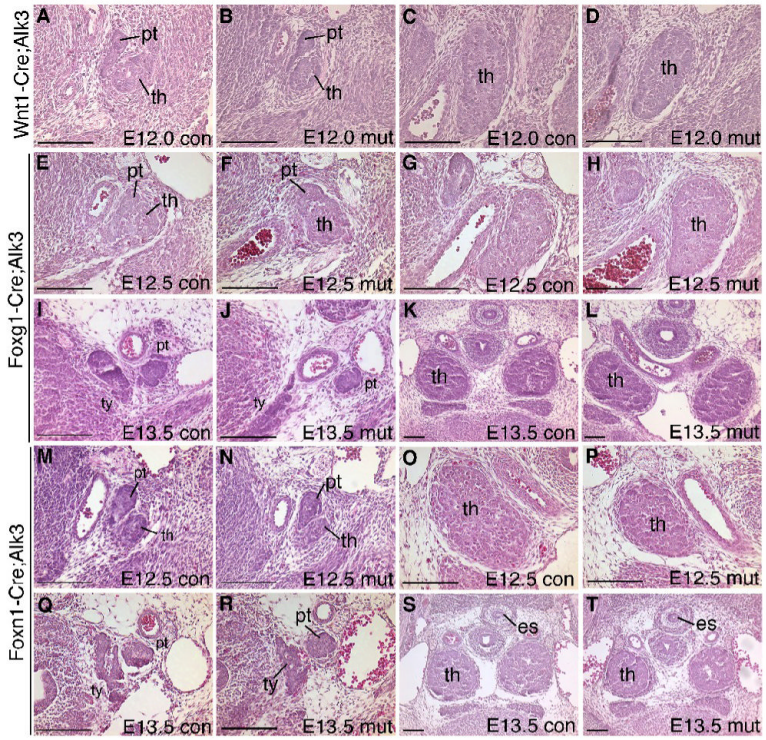

Fig. 9.

Deletion of Bmp4 from neural crest cells or thymic epithelial cells has no effect on early thymus-parathyroid development. Transverse sections through the thymus and parathyroid stained with H&E. (A-F) Wnt1-Cre;Bmp4 mutants and controls at E12.5 (A,D) and E14.5 (B,C,E,F) showing no difference in thymus and parathyroid morphology. At E12.5 the thymus and parathyroid are separate but are still closely associated (A,D). At E14.5 the parathyroids are close to the thyroid (B,E) and the thymus lobes have migrated posteriorly and towards the midline (C,F). (G-J) Foxn1-Cre;Bmp4 mutant and control. The parathyroid in the mutant (I) is adjacent to the thyroid as in the control (G) and there is no difference in the size or location of the thymus (H,J). es, esophagus. th, thymus. pt, parathyroid. ty, thyroid. con, control. mut, mutant. All scale bars = 100μm.

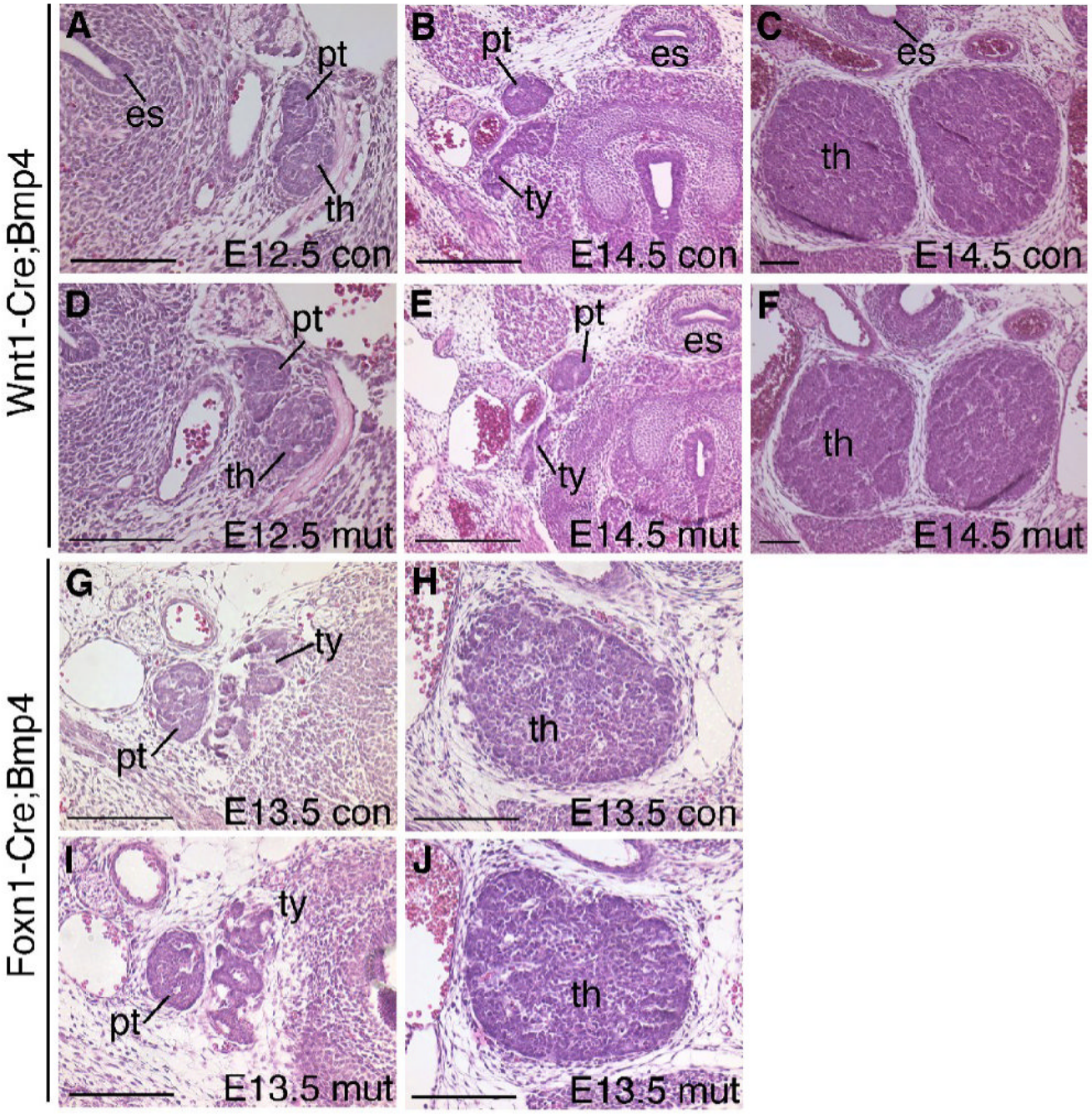

Fig. 10.

Deletion of Alk3 from epithelial and/or mesenchymal cells. H&E stained transverse sections through the thymus and parathyroids. (A-D) Wnt1-Cre;Alk3 control (A,C) and mutant (B,D) embryos at E12.0. (E-H) E12. 5 Foxg1-Cre;Alk3 control (E,G) and mutant (F,H) embryos. (I-L) E13. 5 Foxg1-Cre;Alk3 control (I,K) and mutant (J,L) embryos. (M-T) Foxn1-Cre;Alk3 mutants and controls at E12.5 (M-P) and E13.5 (Q-T). es, esophagus. th, thymus. pt, parathyroid. ty, thyroid. con, control. mut, mutant. All scale bars = 100μm.

Dev Biol. Author manuscript; available in PMC 2011 March 1.

Table 1

	Cre expression		Organ specification	Thymus size	Parathyroid size	Organ separation	Thymus location	Thymus capsule	Embryonic lethal?
	Epithelium	**NC derived mesenchyme**							
Foxg1$^{Cre/+}$; Bmp4$^{-/fx}$	early[a]	early[a]	normal	small	normal	delayed	ectopic (anterior)	partially disrupted	E14.0 – E14.5
Wnt1$^{Cre/+}$; Bmp4$^{-/fx}$	–	+	normal	normal	normal	normal	normal	normal	no
Foxn1$^{Cre/+}$; Bmp4$^{-/fx}$	late[a]	–	normal	normal	normal	normal	normal	normal	no
Foxg1$^{Cre/+}$; Alk3$^{-/fx}$	early[a]	early[a]	normal	small	normal	normal	normal	normal	variable after E11.5[2]
Wnt1$^{Cre/+}$; Alk3$^{-/fx}$	–	+	normal	small	normal	normal	normal	normal	E12.5[1]
Foxn1$^{Cre/+}$; Alk3$^{-/fx}$	late[a]	–	normal	small	normal	normal	normal	normal	no

[a] early and late refer to before or after Foxn1 induction at E11.25, respectively.

+ expressed

– not expressed.

[1] Stottmann et al. 2004.

[2] Hebert et al. 2002.